Tendon and pressure actuation for a bio-inspired manipulator based on an antagonistic principle

Farahnaz Maghooa, Agostino Stilli, Yohan Noh, Kaspar Althoefer, *Member, IEEE* and Helge A Wurdemann

***Abstract*— This paper proposes a soft, inflatable manipulator that is antagonistically actuated by tendons and pneumatics. The combination of the two actuation mechanisms in this antagonistic robot structure is inspired by the octopus which uses its longitudinal and transversal muscles to steer, elongate, shrink and also stiffen its continuum arms. By "activating" its antagonistic muscle groups at the same time, the octopus can achieve multiple motion patterns as well as stiffen their arms. Being organized in a similar fashion, our robot manipulator uses, on the one hand, pneumatic actuation and, on the other hand, tendon-based actuation - one opposing the other, achieving an overall antagonistic actuation framework. Controlling the pressure inside the robot while at the same time controlling the tendons' displacements, the robot can be moved into a wide range of configurations while simultaneously controlling the arm's stiffness. This paper builds on earlier work by the authors: Here, we present a new conic-shaped manipulator structure and the control architecture. Using a constant curvature model, we have derived an approach suitable for controlling the robot manipulator. The manipulator's reachable workspace is analyzed and proof-of-concept experiments were conducted to show the robot's stiffness control and motion abilities.**

I. INTRODUCTION

Nature has inspired researchers to overcome limitations of traditional rigid robots composed of joints and links. In particular animals' appendices such as the octopus arm or the elephant trunk have been imitated to create robotic manipulators with infinite degrees of freedom (DoFs) [1]. These continuum robots can be classified according to their actuation principle: intrinsic, extrinsic or hybrid actuation [2], [3]. The most commonly used actuation principles of continuum robotic manipulator are tendon-driven (extrinsic) [4]–[8] and pneumatic (intrinsic) [9]–[11]. A combination of these types of actuation principles of soft manipulators have been implemented, e.g. in the KSI tentacle [12] and the Air-Octor [13] and merges the advantages of both principles [14], [15].

*The work described in this paper is partially funded by the Seventh Framework Programme of the European Commission under grant agreement 287728 in the framework of EU project STIFF-FLOP. The research was also partially funded/supported by the National Institute for Health Research (NIHR) Biomedical Research Centre based at Guy's and St Thomas' NHS Foundation Trust and King's College London. The views expressed are those of the authors and not necessarily those of the NHS, the NIHR or the Department of Health.

Farahnaz Maghooa is an engineering student with Polytech UPMC, Paris, France. farah.maghooa@laposte.net

Agostino Stilli, Yohan Noh, Kaspar Althoefer and Helge A Wurdemann are with King's College London, Department of Informatics, Centre for Robotics Research, Strand, London, WC2R 2LS, United Kingdom. agostino.stilli, yohan.noh, k.althoefer, helge.wurdemann@kcl.ac.uk

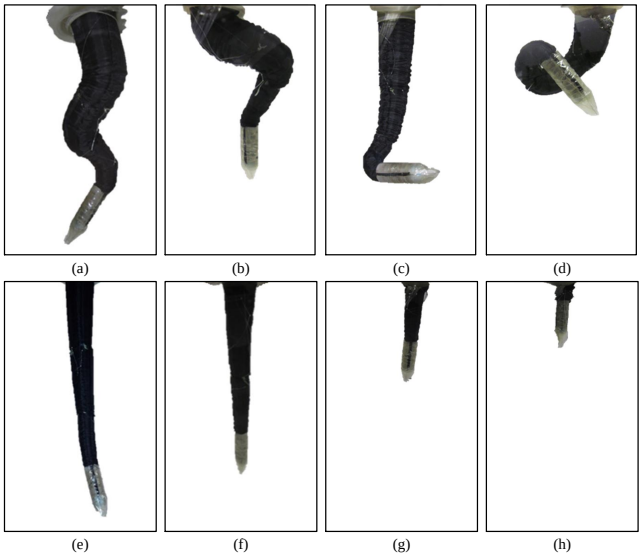

Fig. 1. Examples of possible configurations of the bio-inspired manipulator: actuation of (a) the middle and tip sections, (b) the base and middle sections, (c) the tip section, (d) all sections, and (e)-(h) elongation/shrinkage capability.

A number of continuum robotic manipulators [6], [10] have been designed for surgical applications due to their advantages over traditional robots in terms of compliance and workspace. The infinite degrees of freedom of these types of manipulators have been proven to enhance performance of surgeons during endoluminal procedures like colonoscopy [16] and cardiac surgery [17], [18] as well as for Minimally Invasive Surgery (MIS) [19]. STIFF-FLOP is an EU-FP7 project which, taking inspiration from the octopus arm, aims to combine the advantages of continuum manipulators, that are frequently realized as a sequence of small sized rigid links, with the softness of silicon material to create novel soft continuum manipulators [20] with integrated force [21], [22] and tactile sensors [23]. The current STIFF-FLOP robot prototype consists of a silicon body with three equally spaced hollow chambers embedded within and arranged in a radial fashion along the longitudinal axis; the chambers are pneumatically actuated [20]; Stiffness control is achieved using granular jamming inside an additional chamber within the silicone structure [11].

Researchers have explored actuation principles, where two types have been combined, and concluded that this often leads to enhanced manipulation capabilities [8],

including the advanced control, stiffness and compliance. In [24]–[26], force and position control has been combined to create a hybrid control architecture. Another hybrid robot concept is the one described in [27]; the authors created a system where pneumatic actuators are combined with an electromechanical actuation mechanism. Also, the work by Immegal [12] aims at bringing together extrinsically and intrinsically actuation principles. The idea of fusing pneumatic and tendon-driven actuation was also explored in [10] - in their work, each robot segment is made up of a pressurizable inner hose inside a surrounding hose and a set of cables attached to aluminum plates at the top and base of each of the many segments. In our previous paper [14], we presented the structure of a soft manipulator with antagonistic actuation - pneumatic and tendon-driven - and highlighted the achievements regarding stiffness.

This paper proposes an actuation strategy for the tendon-driven and pneumatic-actuated soft manipulator (see Figure 1). Section II presents the overall system consisting of the bio-inspired soft manipulator. The mathematical model for tendon actuation based on the constant curvature model is part of Section III. In Section IV, the actuation architecture of the antagonistically actuated manipulator is explained: Tendons are integrated to tele-operate each section, pressure control and the combination of tendon and pressure actuation is implemented to change the length and stiffness of the robot. A number of experiments have been conducted which are described along with the results in Section V. Section VI summarizes the achievements of this paper and presents future works.

II. DESIGN OF THE MANIPULATOR AND SYSTEM INTEGRATION

A. Principle of the Antagonistic Actuation

The implemented antagonistic actuation mechanism combines extrinsic (tendon-driven) and intrinsic (pneumatic) actuation [14], [15]. This actuation principle is used by nature in various ways, e.g. in the octopus arms which have longitudinal and transversal muscles. Activating both sets of muscles increases the arms' stiffness [28], [29]. In octopus arms, biologists speak about the connecting tissue that keeps the muscles of the octopus arms in place, avoiding bulging and allowing the animal to achieve stiffness in their arms (comparable to a tube inside a bicycle tire). A similar behavior is achieved with the hybrid manipulation principle presented here. By fusing the advantages of both actuation types, the stiffness of the soft manipulator can be varied and results in a manipulator which is capable of:

- changing its configuration depending on the number of integrated tendons and, hence, bend around obstacles (see Figures 1(a)-(d)),
- varying its length from being entirely elongated to completely shrunk (see Figures 1(e)-(h)),
- simultaneously varying its stiffness, through the controlled interplay of applied pressure and tendon displacement.

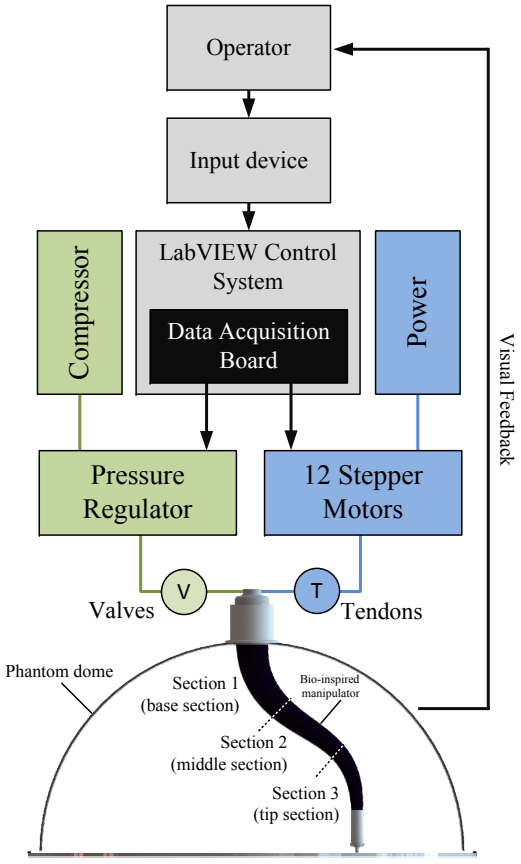

Fig. 2. Conceptual system architecture of the bio-inspired manipulator with three sections and a combination of tendon-driven and pneumatic actuation.

Figure 2 shows the conceptual system architecture of the hybrid actuated manipulator. A human operator will send commands via a joystick (Logic 3 JS282 PC Joystick) and receive visual feedback. Section II-B explains the structural design of the bio-inspired manipulator. In Section 4, the control hardware is described.

B. Design of the Bio-inspired Manipulator with three Sections

3D and section views of the manipulator are shown in Figures 3(a) and (b), respectively. We did not only take inspiration from nature with respect to the antagonistic actuation principle but also regarding the design of the manipulator. As Figure 3 illustrates, the geometric structure can be described as a frustum of a cone (truncated cone). The diameter of the manipulator is 40 mm at the base and narrows down to 10 mm at the tip similar to the shape of an octopus arm.
The robot is composed of three main components: an inner air-tight and stretchable latex bladder, an outer, non-stretchable (but foldable) polyester fabric sleeve and 12 nylon tendons. The stretchable cylindrical latex bladder is inserted into the cylindrical polyester sleeve. The outer sleeve is 30 cm in length, when fully inflated. As the fabric material is non-stretchable, the outer sleeve prevents any ballooning of the inner bladder in radial direction beyond the maximum

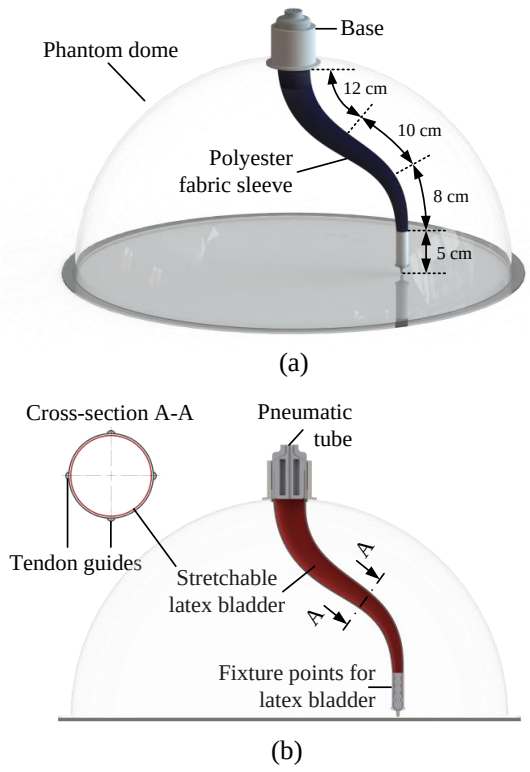

Fig. 3. CAD drawings of the soft manipulator: (a) 3D and (b) section view.

diameter. Whilst morphing from a deflated state to an inflated state, the robot can only expand along its longitudinal axis (elongation). The stiffness of the arm can be controlled by adjusting the tendons appropriately - e.g. tightening the tendons at a fixed air pressure in the sleeve will reduce the robot's length and increase the stiffness. The tip of the latex bladder is mounted to the tip of the outer sleeve to prevent the latex sleeve from twisting inside the manipulator when actuated. The nylon tendons are guided along the outside of the manipulator sleeve within polyester channels, 90° spaced apart along the perimeter of the outer sleeve (as shown in Figure 3(b)). In our three-section prototype, four tendons are fixed to the tip of the manipulator and another two sets of four tendons are attached to the tip of the proximal section. Hence, the base section is 12 cm, the middle section has a length of 10 cm, and the tip section is 8 cm. Employing this approach, the robot's three sections can be independently controlled, Figures 2 and 3.

C. System Integration and Control Hardware

Figure 4 shows the setup of the overall system. The soft manipulator is mounted inside a phantom dome. The 12 tendons that are connected to the three sections are fed through Bowden cables before being wound around a pulley system of 14 mm radius. Each pulley is fixed onto the shaft of a stepper motor (Soyo SY57ST56-0606B Unipolar Stepper Motor). The motors are able to produce a holding torque of 0.6 Nm, have a resolution of 1.8°/step (which has been reduced to $\frac{1}{10}$ of a step using microstepping control), and a precision of ±5 %. By controlling the angular position of the pulley system, it is possible to vary the length of each tendon separately and, hence, the bending of the manipulator. The stepper motors are connected to bi-polar microstepping drivers (Sparkfun Big Easy Driver ROB-11876).
The inner latex bladder is connected to one pressure regulator (SMC ITV0010-3BS-Q). The regulator is able to control the air pressure from 0.001 MPa to 0.1 MPa capable of inflating and deflating the inner bladder of the robot. An in-built pressure sensor ensures to maintain the desired pressure inside the bladder. An air compressor (BAMBI MD Range Model 150/500) ensures the supply with sufficient pressure limited to the maximum pressure the regulators can cope with.
The motor drivers and pressure regulator are interfaced via three DAQ cards (NI USB-6211) to LabVIEW software. A joystick (Logic 3 JS282 PC Joystick) is utilized as a input device for the operator in order to remote-control the position and configuration of the manipulator.

III. MATHEMATICAL APPROXIMATION

A. Constant Curvature Model

The bio-inspired manipulator presented in this paper is composed of three sections which can be configured independently. Figure 5 shows experimental results of the bending behavior of the base section. Multiple bending angles are achieved by actuating one tendon at a time while keeping the pressure constant. The red circles of different diameters in Figure 5 indicate that the manipulator meets the constant curvature condition.
In [30], Webster and Jones presented the kinematics for this type of continuum manipulators. Hence, the geometry can be modeled by the three arc parameters l, ϕ, γ, where l is the arc length, ϕ is the angle defining the plane containing the arc and γ is the curvature of the arc [30]. According to this model, the motion of the robot sections can be decomposed into a rotation of an angle ϕ about the z-axis and a rotation about the direction perpendicular to the plane containing the

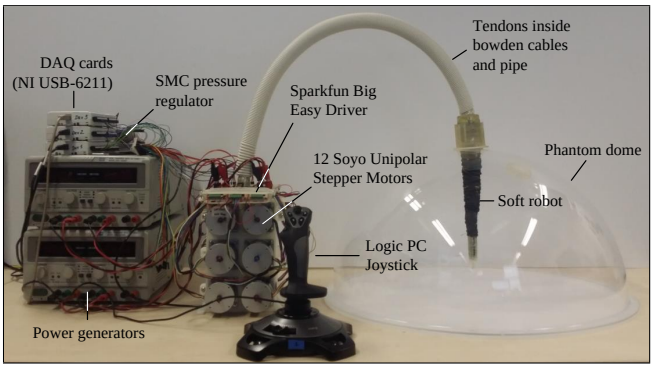

Fig. 4. Setup of the overall system: robotic manipulator inside a phantom dome, Soyo Unipolar Stepper Motors, SMC pressure regulator, Sparkfun Big Easy Drivers, and NI DAQ cards.

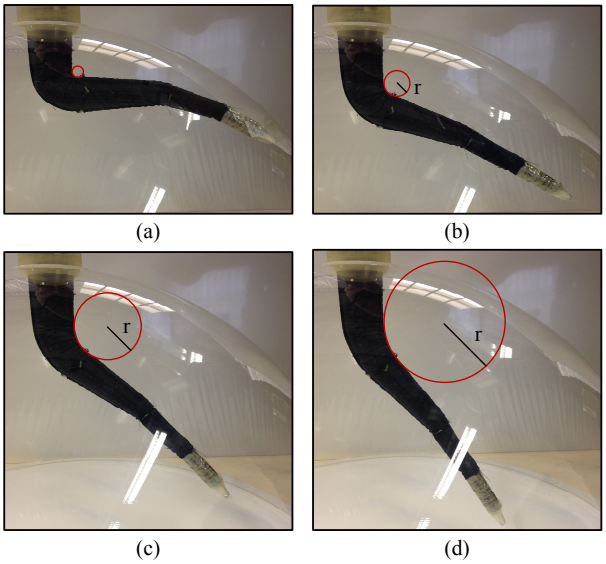

Fig. 5. Bending behavior of the base section in one plane actuating a single tendon.

arc. The transformation matrix $\mathbf{T}$ yields:

$$\mathbf{T} = \begin{pmatrix} \cos\phi\cos\gamma l & -\sin\phi & \cos\phi\sin\gamma l & \frac{\cos\phi(1-\cos\gamma l)}{\gamma} \\ \sin\phi\cos\gamma l & \cos\phi & \sin\phi\sin\gamma l & \frac{\sin\phi(1-\cos\gamma l)}{\gamma} \\ -\sin\gamma l & 0 & \cos\gamma l & \frac{\sin\gamma l}{\gamma} \\ 0 & 0 & 0 & 1 \end{pmatrix} \tag{1}$$

B. Implementation of Mathematical Model

Each section of the manipulator presented here is connected to four tendons spaced 90° around its central axis as shown in the cross-section of Figure 6(a). By implementing tendon actuation and being able to regulate their length simultaneously, the robot's configuration and tip pose can be tele-operated. The length l of each tendons can be determined by the geometry of the manipulator. The bending direction characterized by the angle ϕ can be determined. Due to

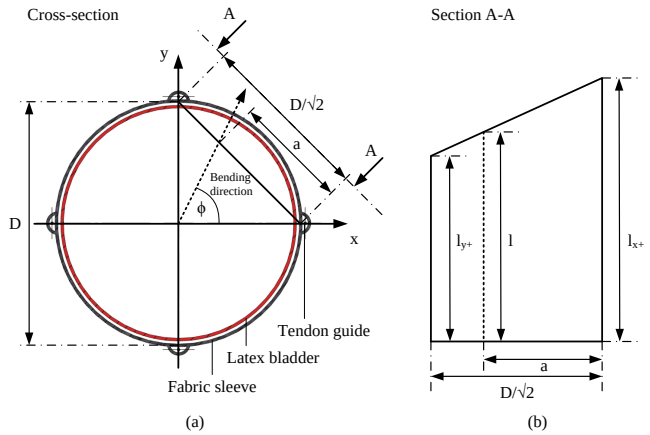

Fig. 6. (a) Cross-section view and (b) section view A-A along the central axis of the manipulator when bending.

the symmetrical arrangement of the tendons, the following description refers to bending angles within the interval $\phi = [0, \frac{\pi}{2}[$. Using trigonometry, an definition of ϕ depending on a and D can be found (see Figure 6(a)).

$$\phi = \arctan\left(-\frac{1}{1-\frac{D}{a\sqrt{2}}}\right) \tag{2}$$

The input device used for the manipulation of the robot relies on position data along the x and y-axis, which corresponding component can be expressed by the bending angle ϕ. Hence, a relation between the length of the tendons and the bending angle is established.

When bending, the section view along the central axis of the manipulator can be approximated by an trapezium as shown in Figure 6(b). For the manipulator's length l, Equation 3 yields:

$$l = \max\left(l_{x+}, l_{y+}\right) + \frac{\sqrt{2}a\left|l_{x+} - l_{y+}\right|}{D} \tag{3}$$

Implementing Equations 2 and 3, it is possible to tele-operate each section of the manipulator.

IV. ACTUATION AND SOFTWARE ARCHITECTURE

The implemented LabVIEW software employs the key characteristics of the manipulator being able to bend, elongate, shrink and stiffen. An open loop control strategy is described here based on the mathematical approximation presented in Section III in order to achieve tendon and pressure actuation and also to fuse both actuation principles to obtain the antagonistic behavior allowing to control the pose and the arm's stiffness (see Figure 2).

Based on the equations described in Section III, tendon actuation is implemented. The length of the tendons is calculated by using the feedback obtained from the 12 stepper motors considering the pulley system of 14 mm radius. Hence, each section of the manipulator can be independently bent in two directions and has two DoFs. An additional DoF is added when all tendons of a section are actuated at the same time and the manipulator elongates or shrinks. The pressure is constant during the tendon-actuated mode and adapts due to feedback from the built-in sensors of the pressure regulators.

In another mode, the internal pressure of the latex bladder can be increased or decreased. Current data from the pressure sensors is used for feedback. In any configuration of the manipulator's sections, the pressure can be changed. Hence, the stiffness of the manipulator can be controlled. Section V shows how the stiffness depends on the internal pressure of the bladder.

The antagonistic principle emerges when pressure and tendon actuation are simultaneously activated so that they complement each other. The combination of intrinsic and extrinsic actuation with our robot structure creates a new type of robotic manipulator that can collapse entirely, extend along its main axis, bend along the main axis and vary its stiffness.

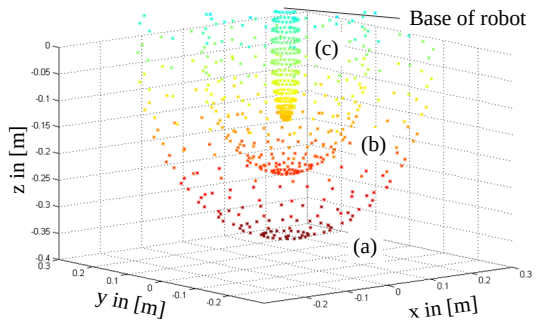

Fig. 7. Simulated workspace of the manipulator with (a) all sections elongated and section 1 actuated, (b) sections 2 and 3 elongated and section 2 actuated, and (c) section 3 elongated and actuated.

V. EXPERIMENTS AND RESULTS

A. The Manipulator's Workspace

Figure 7 illustrates the simulated workspace of the manipulator. The robot is placed upside down - equivalent to the setup presented in Figure 3. Three cases were simulated:

1) All sections are elongated and the base section actuated.
2) The base section was entirely deflated and section 2 actuated.
3) Only section 3 was elongated and actuated.

The results show the volume of the workspace which is limited by the outer hull of a semi-ellipsoid. Any points within this area can be achieved due to the combination of pneumatic and tendon actuation.

B. Stiffness (Force/Stress) Experiments

A series of experiments have been conducted in order to explore the stiffness of the bio-inspired robot. Figure 8 shows the locations where lateral and longitudinal forces were applied.

Lateral forces $F_1, F_2, F_3, F_{\text{Tip}}$ have been exerted along the manipulator at the end of each section and at the tip of the robot. The internal pressure of the bladder was altered from 0.015 MPa to 0.055 MPa and, hence, the stiffness increased. The maximum force held by the robot was defined as a displacement at the tip of 5 mm was reached. The experimental results were recorded and are plotted in Figure 9. The manipulator behaves like a cantilever and is able to hold up to 5.2 N at the tip of section 3.

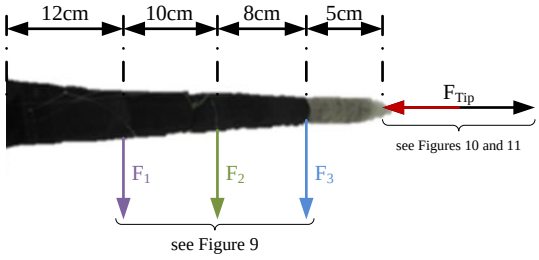

Fig. 8. Experimental stiffness tests with a ATI Nano17 Force/Torque sensor.

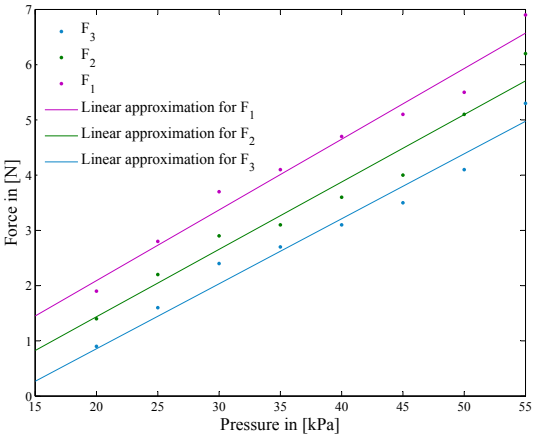

Fig. 9. Experimental results of lateral forces $F_1, F_2, F_3, F_{\text{Tip}}$ applied.

Figure 10 (red curve) shows the results of longitudinal forces actively applied by the manipulator. A ATI Nano 17 Force/Torque sensor was placed at the tip. The internal pressure p was increased and the forces F were measured by the F/T sensor. A polynomial curve was fitted describing the relation between the pressure p and measured force F (see Equation 4).

$$p = -0.0006 \cdot F^2 + 0.0802 \cdot F - 0.4812 \tag{4}$$

It can be noticed that the force F saturates for pressures bigger than $p = 40$ kPa. Hence, there is a limitation of stiffness achieved by the manipulator in longitudinal direction.

The results of a similar experiment are plotted in Figure 11. Here, the tip of the manipulator was displaced by a motorized linear module keeping constant pressure values during each test. The experiment was repeated for pressure values of $p = 15, 30, 40, 55$ kPa. The black curve of Figure 10 records the largest force values achieved at a displacement of 50 mm. The data is fitted by a polynomial curve which is similar to the red curve for pressures $p \leq 40$ kPa:

$$p = -0.0008 \cdot F^2 + 0.0800 \cdot F - 0.2526 \tag{5}$$

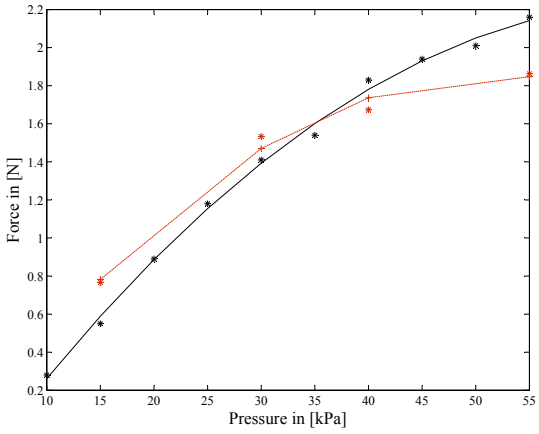

Fig. 10. Longitudinal forces applied to a ATI Nano 17 Force/Torque sensor.

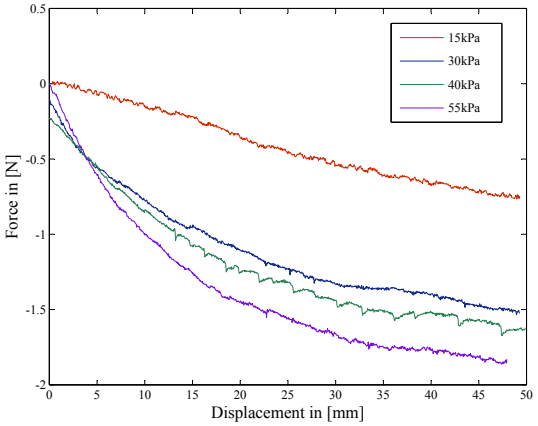

Fig. 11. Displacement tests at the tip of the manipulator using a motorized linear module with a mounted ATI Nano 17 Force/Torque sensor.

VI. CONCLUSIONS

We have presented here work on our new hybrid and antagonistic actuation system for a bio-inspired manipulator fusing pneumatic with tendon-driven actuation building on [14]. In particular, the robot has now a conic shape of 30 cm length being close to the shape of an octopus arm and also allowing the entire manipulator to shrink more effectively. Three sections are integrated actuated by 12 tendons and one internal pressure bladder. Being inspired by the biological role model, the octopus, our antagonistic actuation system aims at modeling the octopus way of using its longitudinal and transversal muscles in its arms: activating both types of muscles, the octopus can achieve a stiffening of its arms. This approach has been implemented in an advanced actuation architecture. Further, we modelled the curvature of each actuated section, simulated the resulting workspace and conducted stiffness experiments.

In future works, the structure of the current manipulator will be enhanced by creating multiple independently stiffness-controllable sections. We will also explore ways to utilize the empty space within the air-filled latex bladder, as possibly required when integrating sensors or actuators for additional tools such as tip-mounted grippers.

REFERENCES

[1] I. Walker, D. Dawson, T. Flash, F. Grasso, R. Hanlon, B. Hochner, W. Kier, C. Pagano, C. Rahn, and Q. Zhang, "Continuum robot arms inspired by cephalopods," in *Unmanned Ground Vehicle Technology VII*, 2005.

[2] G. Robinson and J. Davies, "Continuum robots - a state of the art," in *IEEE International Conference on Robotics and Automation*, 1999.

[3] D. Trivedi, C. Rahn, W. Kier, and I. Walker, "Soft robotics: Biological inspiration, state of the art, and future research," *Applied Bionics and Biomechanics*, vol. 5, no. 2, pp. 99–117, 2008.

[4] R. Cieslak and A. Morecki, "Elephant trunk type elastic manipulator - a tool for bulk and liquid type materials transportation," *Robotica*, vol. 17, pp. 11–16, 1999.

[5] C. Li and C. Rahn, "Design of continuous backbone, cable-driven robots," *ASME Journal of Mechanical Design*, vol. 124, no. 2, p. 265271, 2002.

[6] R. Buckingham, "Snake arm robots," *Industrial Robot: An International Journal*, vol. 29, no. 3, p. 242245, 2002.

[7] D. Camarillo, C. Milne, C. Carlson, M. Zinn, and J. Salisbury, "Mechanics modeling of tendon-driven continuum manipulators," *IEEE Transactions on Robotics*, vol. 24, no. 6, pp. 1262–1273, 2008.

[8] I. D. Walker, "Robot strings: Long, thin continuum robots," in *IEEE Aerospace Conference*, 2013.

[9] S. Neppalli, B. Jones, W. McMahan, V. Chitrakaran, I. Walker, M. Pritts, M. Csencsits, C. Rahn, and M. Grissom, "Octarm - a soft robotic manipulator," in *IROS*, 2007.

[10] B. Jones, W. McMahan, and I. Walker, "Design and analysis of a novel pneumatic manipulator," in *IFAC Symposium "Advances in Automotive Control"*, 2004.

[11] A. Jiang, E. Secco, H. Wurdemann, T. Nanayakkara, P. Dasgupta, and K. Athoefer, "Stiffness-controllable octopus-like robot arm for minimally invasive surgery," in *3rd Joint Workshop on New Technologies for Computer/Robot Assisted Surgery*, 2013.

[12] G. Immega and K. Antonelli, "The KSI tentacle manipulator," in *IEEE International Conference on Robotics and Automation*, 1995.

[13] W. McMahan, B. Jones, and I. D. Walker, "Design and implementation of a multi-section continuum robot: Air-octor," in *IEEE/RJS International Conference on Intelligent Robots and Systems*, 2005.

[14] A. Stilli, H. Wurdemann, and K. Althoefer, "Shrinkable, stiffness-controllable soft manipulator based on a bio-inspired antagonistic actuation principle," in *IROS*, 2014.

[15] A. Stilli, F. Maghooa, H. Wurdemann, and K. Althoefer, "A new bio-inspired, antagonistically actuated and stiffness controllable manipulator," in *Workshop on Computer/Robot Assisted Surgery*, 2014.

[16] G. Chen, M. Pham, T. Herve, and C. Prelle, "Design and modeling of a micro-robotic manipulator for colonoscopy," in *International Workshop on Research and Education in Mechatronics*, 2005.

[17] A. Ataollahi, R. Karim, A. S. Fallah, K. Rhode, R. Razavi, L. Seneviratne, T. Schaeffter, and K. Althoefer, "3-dof mr-compatible multi-segment cardiac catheter steering mechanism," *IEEE Transactions on Biomedical Engineering*, vol. 99, 2013.

[18] Y. Bailly and Y. Amirat, "Modeling and control of a hybrid continuum active catheter for aortic aneurysm treatment," in *ICRA*, 2005.

[19] J. Shang, D. Noonan, C. Payne, J. Clark, M. Sodergren, A. Darzi, and G.-Z. Yang, "An articulated universal joint based flexible access robot for minimally invasive surgery," in *International Conference on Robotics and Automation*, pp. 1147–1152, 2011.

[20] M. Cianchetti, T. Ranzani, G. Gerboni, I. de Falco, C. Laschi, and A. Menciassi, "Stiff-flop surgical manipulator: Mechanical design and experimental charaterization of the single module," in *IEEE/RSJ International Conference on Intelligent Robots and Systems*, 2013.

[21] Y. Noh, S. Sareh, J. Back, H. Wurdemann, T. Ranzani, E. Secco, A. Faragasso, H. Liu, and K. Althoefer, "A three-axial body force sensor for flexible manipulators," in *IEEE International Conference on Robotics and Automation*, 2014.

[22] Y. Noh, E. Secco, S. Sareh, H. Wurdemann, A. Faragasso, J. Back, H. Liu, E. Sklar, and K. Althoefer, "A continuum body force sensor designed for flexible surgical robotic devices," in *IEEE Engineering in Medicine and Biology Society*, 2014.

[23] S. Sareh, A. Jiang, A. Faragasso, Y. Noh, T. Nanayakkara, P. Dasgupta, L. Seneviratne, H. Wurdemann, and K. Althoefer, "Bio-inspired tactile sensor sleeve for surgical soft manipulators," in *ICRA*, 2014.

[24] T. Yoshikawa, "Dynamic hybrid position/force control of robot manipulators-description of hand constraints and calculation of joint driving force," *IEEE J. Robot. Automat.*, vol. 3, no. 5, 1987.

[25] M. Branicky, V. Borkar, and S. Mitter, "A unified framework for hybrid control: Model and optimal control theory," *IEEE Transactions on Automation Control*, vol. 43, no. 1, 1998.

[26] M. Parnichkun and C. Ngaecharoenkum, "Kinematics control of a pneumatic system by hybrid fuzzy pid," *Mechatronics*, vol. 11, no. 8, pp. 1101–1023, 2001.

[27] D. Shin, I. Sardellitti, and O. Khatib, "A hybrid actuation approach for human-friendly robot design," in *IEEE International Conference on Robotics and Automation*, pp. 1747–1752, 2008.

[28] Y. Gutfreund, T. Flash, G. Fiorito, and B. Hochner, "Patterns of arm muscle activation involved in octopus reaching movements," *The Journal of Neuroscience*, vol. 18, no. 15, p. 5976598, 1998.

[29] C. Laschi, B. Mazzolai, V. Mattoli, M. Cianchetti, and P. Dario, "Design of a biomimetic robotic octopus arm," *Bioinspiration and Biomimetics*, vol. 4, pp. 1–8, 2009.

[30] R. Webster III and B. Jones, "Design and kinematic modeling of constant curvature continuum robots: A review," *The International Journal of Robotics Research*, 2010.